

Optimal pump frequency for ac hysteretic SQUID

Andrey L. Pankratov*

Institute for Physics of Microstructures of RAS, Nizhny Novgorod, Russia

(Received 28 October 2002; revised manuscript received 14 February 2003; published 11 July 2003)

The recently discovered effect of suppression of noise by a strong periodic signal is observed and investigated in the model of real electronic device, representing an ac hysteretic superconducting quantum interference device (SQUID). This effect is characteristic for any electronic device of the trigger type, where transitions between adjacent states occur dynamically under the influence of a periodic signal. The effect appears as a weak dependence of temporal characteristics on noise intensity in a certain range of the pump signal frequency and through the existence of a signal-to-noise ratio maximum as a function of this frequency. The specific feature of the SQUID is the weak dependence of the voltage-flux characteristic on noise intensity in a certain range of parameters. The utilization of this effect by proper tuning the system parameters allows one to significantly improve the SQUID sensitivity.

DOI: 10.1103/PhysRevB.68.024503

PACS number(s): 85.25.Dq, 74.40.+k

I. INTRODUCTION

The ac hysteretic superconducting quantum interference device (ACH SQUID) is a Josephson junction (JJ), enclosed by a superconducting ring and coupled to a microwave resonator¹⁻³ (the conventional setup is presented in Fig. 1). This system is multistable and exhibits very rich dynamics, therefore it has been investigated for many years, and recently phenomena such as stochastic resonance⁴ and nonlinear multilevel dynamics⁵ have been observed there. However, the main utilization of the ACH SQUID is magnetometry (a SQUID allows one to measure magnetic fields less than the flux quantum $\Phi_0 = h/2e$) and in this respect most of the studies were performed.⁶⁻⁹ It is well known that the factor limiting the flux sensitivity of the SQUID is noise,⁶⁻⁸ but an increase in the pump frequency of the tank circuit may improve noise properties of the device. However, due to mathematical difficulties, the studies have been carried out only in the low- and high-frequency limits, and still one is unaware that at which pump frequency the ACH SQUID should operate to demonstrate maximal sensitivity. Recently, the effect of suppression of noise by a strong periodic signal has been observed in a model bistable system.¹⁰ This effect is characteristic for any electronic device of the trigger type, where transitions between adjacent states occur dynamically under the influence of a periodic signal and where noise is only a minor disturbing factor leading to noise-induced errors.

The present paper is devoted to a theoretical investigation of the effect of suppression of noise in a model describing the real electronic device (ac hysteretic SQUID), with the aim to show that how the utilization of this effect may allow one to reduce noise-induced errors in the system. The practical usefulness of the performed study is the recommendation that at which parameters the ACH SQUID should operate to demonstrate maximal sensitivity.

II. SETUP OF THE PROBLEM AND MAIN RESULTS

The theory of an ACH SQUID is already quite well developed (see, e.g., Refs. 1-3 and references therein). Necessary requirements for the SQUID's operating in a hysteretic

mode are the following: $\ell \geq 1$ to provide hysteresis and maximize nonlinearity [where $\ell = L/L_0$, L is the inductance of the ring, $L_0 = \Phi_0/(2\pi I_c)$, I_c is the critical current of the JJ, and Φ_0 is the flux quantum] and $\beta = 2\pi I_c R_N^2 C/\Phi_0 \ll 1$ (the SQUID should be overdamped) to prevent from stochasticity when switching between states with different trapped fluxes in the SQUID ring (here $R_N^{-1} = G_N$ is the normal conductivity of the JJ and C is the capacitance).

The fluctuational dynamics of a flux in a SQUID ring coupled to a resonator may be described by the following equations:

$$\dot{\varphi} + \ell \sin \varphi + \varphi - \varphi_m - \alpha_s \psi(t) = \varphi_F(t), \quad (1)$$

$$\frac{1}{\omega_0^2} \ddot{\psi} + \frac{\eta_r}{\omega_0} \dot{\psi} + \psi = \alpha_r (\varphi - \varphi_m) + a \sin(\omega_0 t). \quad (2)$$

Here, $\varphi = 2\pi\Phi/\Phi_0$, Φ is the trapped flux, $\varphi_m = 2\pi\Phi_m/\Phi_0$, Φ_m is the measured flux, and $\psi(t)$ is the pump signal from the resonator; time is normalized to the characteristic frequency of the SQUID, $\omega_s = \omega_c/\ell = R_N/L$, $\omega_c = 2\pi R_N I_c/\Phi_0$ is the characteristic frequency of the JJ, η_r is the damping of the resonator, α_s and α_r are coupling coefficients of the SQUID ring and the resonator, respectively, and $\omega_0 = \omega_r/\omega_s$ is the dimensionless pump frequency.

Let us take into account only internal thermal fluctuations in the SQUID ring. In this case, the noise source $\varphi_F(t)$ may be represented by the white Gaussian noise,

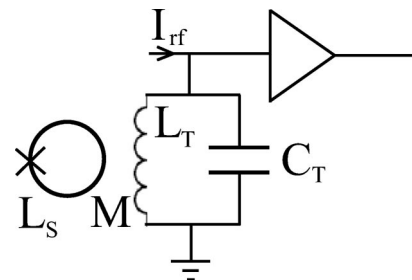


FIG. 1. The conventional setup of an ac hysteretic SQUID; L_S is the SQUID ring inductance, L_T and C_T are inductance and capacitance of the tank circuit, and M is the mutual inductance.

$$\langle \varphi_F(t) \rangle = 0, \quad \langle \varphi_F(t) \varphi_F(t + \tau) \rangle = 2\gamma\ell \delta(\tau), \quad (3)$$

where $\gamma = 2\pi k_B T / (\Phi_0 I_c)$ is the dimensionless noise intensity, T is the temperature, and k_B is the Boltzmann constant.

Let us first consider analytically and numerically the fluctuational flux dynamics of a SQUID ring, assuming that the signal from the resonator is known: $\alpha_s \psi(t) = A \sin(\omega_0 t + \xi)$, where A is the driving amplitude and ξ is the initial phase. In this case, the required statistical characteristics may be computed on the basis of the transitional probability density $W(\varphi, t)$. It is well known that the Fokker-Planck equation for the probability density $W(\varphi, t)$ corresponds to Eq. (1) for the flux:

$$\begin{aligned} \frac{\partial W(\varphi, t)}{\partial t} = & - \frac{\partial G(\varphi, t)}{\partial \varphi} = \frac{\partial}{\partial \varphi} \left\{ \left[\frac{du(\varphi, t)}{d\varphi} W(\varphi, t) \right] \right. \\ & \left. + \gamma\ell \frac{\partial W(\varphi, t)}{\partial \varphi} \right\}, \end{aligned} \quad (4)$$

where

$$u(\varphi) = -\ell \cos(\varphi) + (\varphi - \varphi_e)^2/2 \quad (5)$$

is the dimensionless potential profile and $\varphi_e = \varphi_m + A \sin(\omega_0 t + \xi)$ is the external flux. The initial and boundary conditions for Eq. (4) are

$$W(\varphi, 0) = \delta(\varphi - \varphi_0) \quad \text{and} \quad G(\pm\infty, t) = 0.$$

The quantity that characterizes the noise-induced transition process from the metastable state is a probability $P(t) = \int_{-\infty}^d W(\varphi, t) d\varphi$ that a transition will not occur at the moment of time t (the survival probability), where d is some boundary point, usually a potential barrier top.

To describe analytically the survival probability one can recourse to the adiabatic approximation, which for the case of a weak driving has been used for the description of ACH SQUID (Ref. 6) and in the context of stochastic resonance.^{4,11} It has been demonstrated in Ref. 12 (see also Ref. 13) that for the case of a metastable potential and a strong periodic driving, the evolution of survival probability in the frequency range $0 \leq \omega_0 < 0.5$ may be well described by a modified adiabatic approximation, which allows one to extend the usual analysis to arbitrary driving amplitudes and noise intensities. For simplicity, let us consider the case for $\varphi_m = \pi$ (bistable potential), then the survival probability may be written in the form

$$\begin{aligned} P(\varphi_0, t) = & g(t) \left[P(\varphi_0, 0) + \int_0^t \frac{dt'}{g(t') \tau_q(\varphi_0, t')} \right], \\ g(t) = & \exp \left\{ - \int_0^t \left[\frac{1}{\tau_p(\varphi_0, t')} + \frac{1}{\tau_q(\varphi_0, t')} \right] dt' \right\}, \end{aligned} \quad (6)$$

where $\tau_p(\varphi_0, t')$ is the exact mean decay time of the left metastable state obtained for the corresponding time-constant potential:^{13,14}

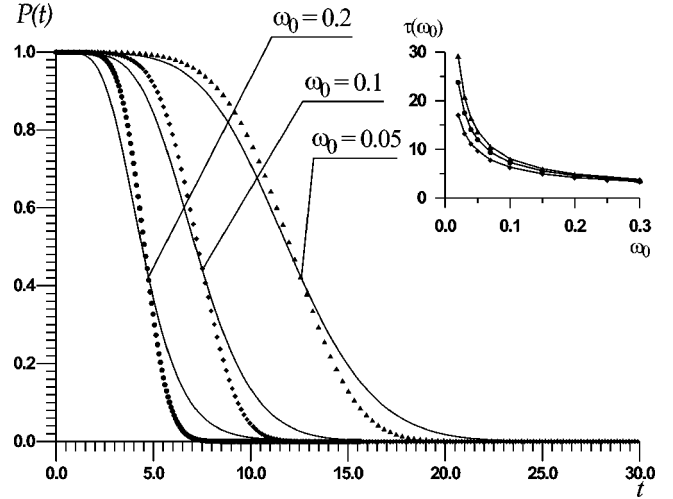


FIG. 2. The evolution of survival probability; dots—computer simulations and solid line—modified adiabatic approximation. Inset: the mean transition time; dots—computer simulations and solid line—modified adiabatic approximation; $\gamma = 0.04, 0.1, 0.2$ from top to bottom.

$$\begin{aligned} \tau_p(\varphi_0) = & \frac{1}{\gamma\ell} \left\{ \int_{\varphi_0}^d e^{u(y)/\gamma\ell} \int_{-\infty}^y e^{-u(x)/\gamma\ell} dx dy \right. \\ & \left. + \int_d^c e^{u(y)/\gamma\ell} dy \int_{-\infty}^d e^{-u(x)/\gamma\ell} dx \right\}. \end{aligned} \quad (7)$$

Here, $c > d$ is the coordinate of the right potential minimum at the moment when $\sin(\omega_0 t + \xi) = 1$ and the left minimum disappears. The time scale τ_q is the decay time of the right metastable state and is calculated from the same formula (7) where in potential (5) the phase of the driving signal is changed from 0 to π . Note that with respect to the usual adiabatic analysis the approximate Kramers' time has been substituted by the exact one (7) and a surprisingly good agreement of this approximate expression with the computer simulation results has been found in a rather broad range of parameters, which is seen in Fig. 2.

In Fig. 2 the probability evolution is presented for $\gamma = 0.1$, $A = 3$, $\xi = 0$, and $\varphi_m = \pi$. The adiabatic approximation is drawn by a solid line, while the results of numerical solution of Eq. (4) by dots. One can see that the coincidence is good enough. An even better agreement between the modified adiabatic approximation (6) and (7) and the computer simulation results may be observed for the mean decay time of the left metastable state (inset of Fig. 2). Since the working conditions for the considered potential are such that during half of the driving period T_ω the survival probability monotonically changes from unity to almost zero, we can define the mean decay time in the time-periodic potential as

$$\tau_p(\omega_0) = \frac{\int_0^{T_\omega/2} [P(t) - P(0)] dt}{P(T_\omega/2) - P(0)}. \quad (8)$$

Definition (8) is analogous to the widely used definition of integral relaxation time for diffusion in time-constant poten-

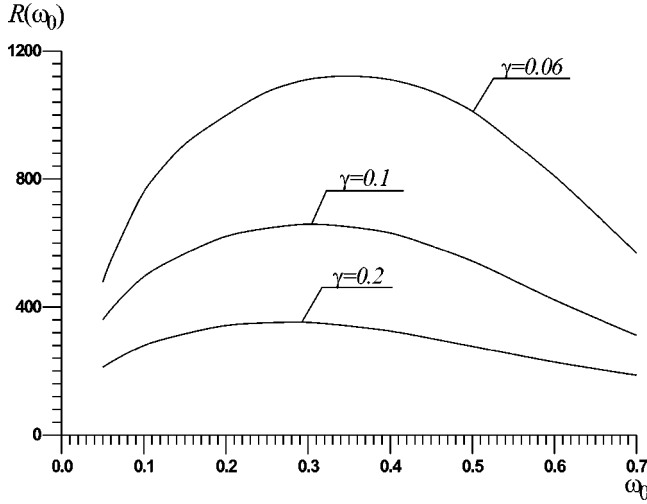


FIG. 3. The signal-to-noise ratio as a function of driving frequency.

tials (see Ref. 13, and references therein). As it is seen from the inset of Fig. 2, in the range of validity of adiabatic approximation the mean decay time (8) computed using formulas (6) and (7) gives perfect coincidence with the results of computer simulation. It is intriguing to see that there is a range of driving frequencies $0.1 \leq \omega_0 \leq 0.3$, where the mean decay time is almost insensitive to the noise intensity: the curves for different noise intensities actually coincide, which constitutes the effect of suppression of noise by a strong periodic signal. This effect may also be demonstrated by the analysis of the signal-to-noise ratio R . In accordance with Ref. 4 we denote R as

$$R = \frac{1}{S_N(\omega_0)} \lim_{\Delta\omega \rightarrow 0} \int_{\omega_0 - \Delta\omega}^{\omega_0 + \Delta\omega} S(\omega) d\omega, \quad (9)$$

where $S(\omega) = \int_{-\infty}^{+\infty} e^{-i\omega\tau} K[\tau] d\tau$ is the spectral density, $S_N(\omega_0)$ is noisy pedestal at the driving frequency ω_0 , and $K[\tau] = \langle\langle \varphi(t+\tau)\varphi(t) \rangle\rangle$, where the inner brackets denote the ensemble average and outer brackets indicate the average over initial phase ξ . In order to obtain $K[\tau]$, Eq. (4) has been solved numerically for $A=3$, $\ell=3$, and $\varphi_m = \pi$.

Let us plot the signal-to-noise ratio (SNR) as a function of driving frequency ω_0 . From Fig. 3 one can see that R as a function of ω_0 has a pronounced maximum. The location of this maximum lies below the cutoff frequency ($\omega_0 = 1$ or $\omega_s = R_N/L$ in dimensional notations) and depends on the driving amplitude A and noise intensity. The existence of optimal driving frequency may be explained in the following way: with an increase in frequency noise-induced escapes occur at the lower barrier, and the maximum of SNR corresponds to the lowest barrier which is closest to the dynamical case, where the transitions occur when the barrier completely disappears. With a further increase in frequency, there is not enough time for transition in the absence of noise and SNR drops, while the mean transition time rises.^{10,12}

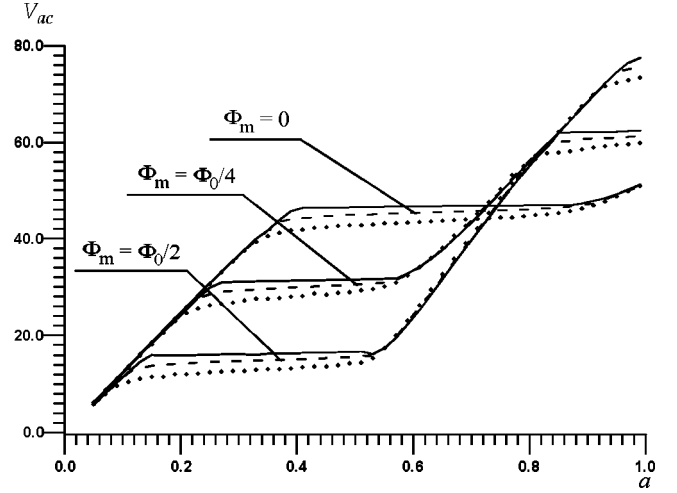


FIG. 4. The ac current-voltage characteristic for $\omega_0 = 0.01$; solid line— $\gamma = 0$, dashed line— $\gamma = 0.01$, and diamonds— $\gamma = 0.03$.

One can solve numerically the system of equations (1) and (2) and compute the ac current-voltage characteristic and the voltage-flux characteristic.

In Fig. 4, the ac current-voltage characteristic [$V_{ac}(a) = \sqrt{2} \psi^2$, $\varphi_m = 0, \pi/2, \pi$; or $\Phi_m = 0, \Phi_0/4, \Phi_0/2$ in dimensional notations) is presented for $\omega_0 = 0.01$ that corresponds to a relatively low-frequency case and for the following parameters: $\ell = 3$, $\eta_r = 0.01$, and $\alpha_s \alpha_r / \eta_r = 2$. As it is seen, for the case $\gamma = 0$ the plateaus are nearly horizontal. For $\gamma = 0.01$ and $\gamma = 0.03$, the plateaus have a tilt and lie below the curves for $\gamma = 0$. The voltage-flux characteristic for the same parameters and $a = 0.47$ is presented in Fig. 5. It is seen that with an increase in noise intensity γ , the corresponding curves move down and their edges are rounded. Low-frequency interference, as well as noise of the resonator and amplifiers (which were not taken into account in the present paper), will make the situation worse and the quantity of splitting of the curves for different γ will give the error of the measured flux φ_m . Fortunately, with the increase in the

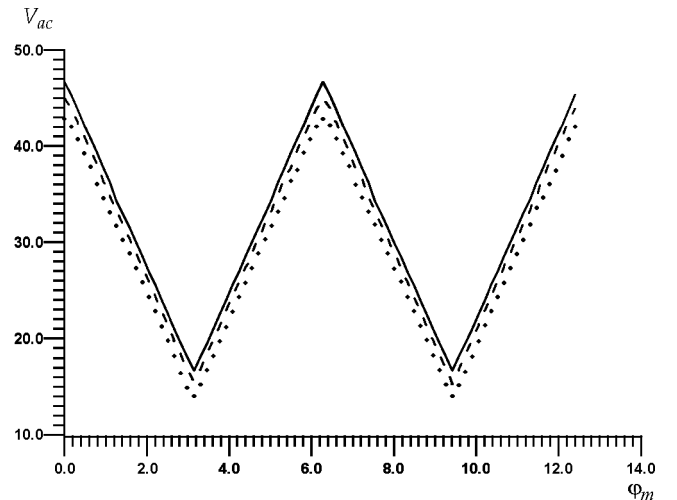


FIG. 5. The voltage-flux characteristic for $\omega_0 = 0.01$; solid line— $\gamma = 0$, dashed line— $\gamma = 0.01$, and diamonds— $\gamma = 0.03$.

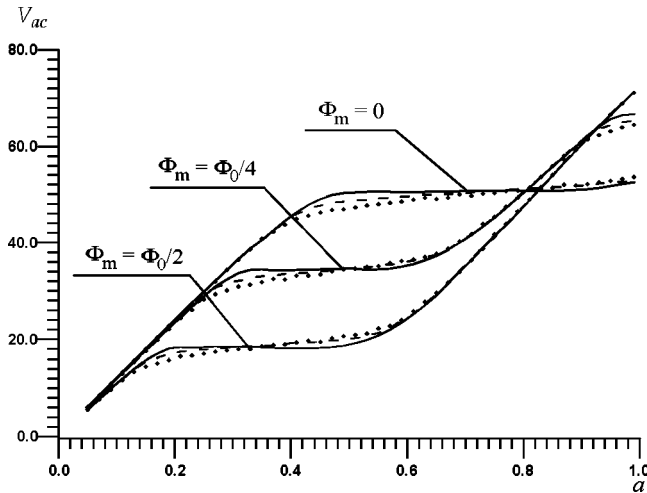


FIG. 6. The ac current-voltage characteristic for $\omega_0=0.3$; solid line— $\gamma=0$, dashed line— $\gamma=0.01$, and diamonds— $\gamma=0.03$.

pump frequency the picture changes radically: already at $\omega_0=0.1$ the plateaus for $\gamma=0.01$ cross the plateaus for $\gamma=0$ at certain points. By approaching the maximum of signal-to-noise ratio $\omega_0 \approx 0.3$ (Fig. 3), the crossing points move to the middle of the plateau and for different γ become more close to each other, see Fig. 6.

It is obvious that to reach the maximal sensitivity of the SQUID, the voltage-flux characteristic should be computed for the pump amplitude a , corresponding to the crossing point of plateaus for $\varphi_m = \pi/2$ (or $\Phi_m = \Phi_0/4$ in dimensional units, see analogous consideration for dc SQUID's in Ref. 15). In Fig. 7, the voltage-flux characteristic is plotted for $\omega_0=0.3$, $a=0.51$, and $\gamma=0, 0.01, 0.03$. It is seen that there is a broad range of φ_m , $0.7 \leq \varphi_m \leq 2.2$, where curves for different γ coincide and, therefore, noise actually does not affect the SQUID in this range of parameters. If, however, the measured flux lies outside this range, some known quantity of magnetic flux φ_n may be added to shift the working point to this region, precise measurements may be performed, and φ_n may be extracted to get information about the original measured flux.

III. CONCLUSIONS

In the present paper the effect of suppression of noise by a strong periodic signal has been observed and investigated in the model of ac hysteretic SQUID. The effect manifests itself in the independence of temporal characteristics on noise intensity in a certain range of frequencies of the pump signal, in the existence of a signal-to-noise ratio maximum as a function of this frequency, and in the weak dependence of the voltage-flux characteristic on noise intensity in a certain range of parameters. In order to reduce noise-induced errors

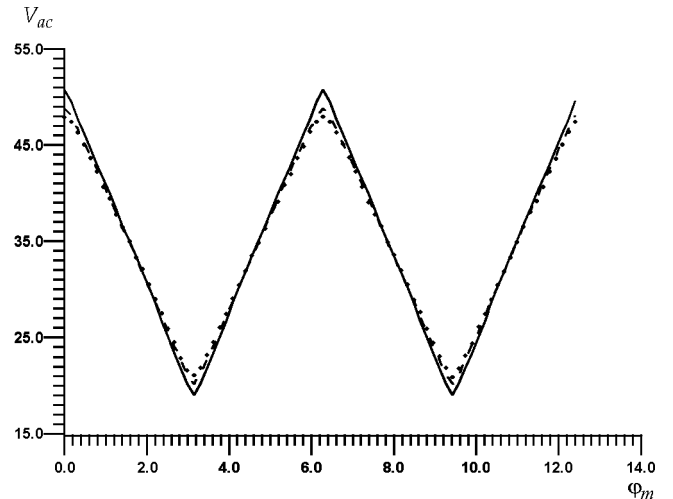


FIG. 7. The voltage-flux characteristic for $\omega_0=0.3$; solid line— $\gamma=0$, dashed line— $\gamma=0.01$, and diamonds— $\gamma=0.03$.

and achieve maximal sensitivity of the SQUID, the following recommendations may be given: the ratio between the pump and the characteristic frequencies $\omega_0 = \omega_r \ell / \omega_c$ must be in the range $\omega_0 \approx 0.2-0.3$ (which in dimensional notations correspond to the condition $\omega_r \approx 0.2R_N/L - 0.3R_N/L$); during measurements, a very important parameter is the amplitude of ac driving that can be chosen from the ac current-voltage characteristic of the SQUID as the point where the plateau for $\Phi_m = \Phi_0/4$ for a given temperature $k_B T \neq 0$ crosses the plateau for $k_B T = 0$. It should be noted that, as calculations for the ACH SQUID system (1) and (2) demonstrate, the signal-to-noise ratio decreases about 5–10 times when changing the dimensionless pump frequency from 0.3 to 0.02. It should be stressed, however, that the analysis is performed only for internal thermal fluctuations and, in practice, the SNR gain may be less than that predicted by the theory due to the effect of resonator and readout electronics fluctuations. Finally, the presented analysis demonstrates, that the improvement of the ACH SQUID sensitivity is possible without changing the conventional setup by a simple adjustment of the SQUID parameters to get the required proportion between the characteristic and the pump frequencies by changing, e.g., R_N/L ratio.

ACKNOWLEDGMENTS

The author wishes to thank V. V. Kurin, Yu. N. Nozdrin, and M. Salerno for helpful discussions. The work has been supported by the Russian Foundation for Basic Research (Project Nos. 03-02-16533, 02-02-16775, 02-02-17517, 03-02-06343, and SS-1729.2003.2) by INTAS (Project Nos. 01-0367 and 01-0450) and by the grant from BRHE and SOC PSNS NNSU.

*Electronic address: alp@ipm.sci-nnov.ru

¹K. K. Likharev, *Dynamics of Josephson Junctions and Circuits* (Gordon and Breach, New York, 1986).

²A. Barone and G. Paterno, *Physics and Applications of the Josep-*

son Effect (Wiley, New York, 1982).

³D. Koelle, R. Kleiner, F. Ludwig, E. Dantsker, and J. Clarke, *Rev. Mod. Phys.* **71**, 631 (1999).

⁴L. Gammaitoni, P. Hanggi, P. Jung, and F. Marchesoni, *Rev. Mod.*

- Phys. **70**, 223 (1998).
- ⁵R.J. Prance, R. Whiteman, T.D. Clark, H. Prance, V. Schollmann, J.F. Ralph, S. Al-Khawaja, and M. Everitt, Phys. Rev. Lett. **82**, 5401 (1999).
- ⁶J. Kurkijarvi, Phys. Rev. B **6**, 832 (1972).
- ⁷V.V. Danilov and K.K. Likharev, Radiotekh. Elektron. (Moscow) **8**, 1725 (1980) [Radio Eng. Electron. Phys. **25**, 112 (1980)].
- ⁸O.V. Snigirev, Radiotekh. Elektron. (Moscow) **10**, 2178 (1981).
- ⁹R.A. Buhrman and L.D. Jackel, IEEE Trans. Magn. **13**, 879 (1977).
- ¹⁰A.L. Pankratov, Phys. Rev. E **65**, 022101 (2002).
- ¹¹B. McNamara and K. Wiesenfeld, Phys. Rev. A **39**, 4854 (1989).
- ¹²A.L. Pankratov and M. Salerno, Phys. Lett. A **273**, 162 (2000).
- ¹³A.N. Malakhov and A.L. Pankratov, Adv. Chem. Phys. **121**, 357 (2002).
- ¹⁴A.N. Malakhov and A.L. Pankratov, Physica C **269**, 46 (1996).
- ¹⁵G.V. Prokopenko, S.V. Shitov, D.V. Balashov, P.N. Dmitriev, V.P. Koshelets, and J. Mygind, IEEE Trans. Appl. Supercond. **11**, 1239 (2001).